

Relativistic Flows at the Hotspots of Radio Galaxies and Quasars?

Markos Georganopoulos and Demosthenes Kazanas

NASA, Goddard Space Flight Center, Code 661, Greenbelt, MD 20771

Abstract

We review the broad band properties of X-ray detected hotspots in radio galaxies and quasars. We show that their collective spectral properties can be unified in a framework involving frequency dependent relativistic beaming and varying orientations to the observer's line of sight. The simplest dynamic model consistent with this picture is a slowing-down relativistic flow downstream from the hotspot shock, suggesting that the jet flows remain relativistic to the hotspot distances.

1 Cygnus A vs. Pictor A

Pairs of radio emitting jets with lengths up to several hundred kpc originate from the central region of radio loud active galaxies. In the most powerful of them, the jets terminate in the hotspots, compact high brightness regions, where the jet collides with the intergalactic medium (IGM). The first hotspots to be detected in X-rays were those of the nearby powerful radio galaxy Cygnus A (1), whose X-ray flux was found in agreement with synchrotron self Compton emission in equipartition between electron and magnetic field energy densities (SSCE). These hotspots show no optical emission, suggesting a spectral cutoff at lower frequencies. While *Chandra* observations of Cygnus A confirmed the SSCE picture (2), observations of Pictor A, another nearby powerful galaxy (3) showed a very different picture: a.) an one-sided large scale X-ray jet on the same direction with the known VLBI jet (4); b.) Detection of X-ray emission only from the hotspot on the jet side, which was also detected in the optical. In addition, SSCE models for the Pictor A hotspots underproduce the observed X-ray flux, requiring a magnetic field ~ 14 times below its the equipartition value in order to achieve agreement with the observed the X-ray flux.

The one-sided X-ray jet of Pictor A suggests the potential importance of relativistic beaming and orientation as a discriminant of the hotspot properties of these two sources. An indicator of orientation is the ratio R of the core

Table 1
Sources with X-ray hotspot detection

Source	Type	Log R	Optical	X-ray	SSCE
3C 330	NLRG	-3.5 (7)	NO	YES (8), 2 sides	YES
Cygnus A	NLRG	-3.3(5)	NO	YES(1; 2) 2 sides	YES
3C 295	NLRG	-2.7(5)	YES	YES (9; 10), 2 sides	YES
3C 123	NLRG	-1.9(11)	NO	YES(12), 1 side	YES
3C 263	Q	-1.0(13)	YES(8), jet side	YES(8), Jet side	See text
3C 351	Q	-1.9(14)	YES(8; 15), jet side	YES(8; 15), jet side	NO
Pictor A	BLRG	-1.2(5)	YES(3), jet side	YES(3), jet side	NO
3C 303	Q	-0.7(5)	YES(16), jet side	YES(17), jet side	NO
3C 390.3	BLRG	-1.1(5)	YES(16; 18), jet side	YES(19), jet side	NO

(beamed) to the extended (isotropic) radio emission. Sources with jets closer to the line of sight are expected to have higher values of R than sources with jets closer to the plane of the sky. Cygnus A has $\log R \approx -3.3$ (5), while Pictor A has $\log R \approx -1.2$ (5), suggesting that the jets of Pictor A are closer to the line of sight than those of Cygnus A. Another indicator of source orientation is the detection of broad emission lines in the optical-UV spectrum of the core of a source. According to the unification scheme for radio loud active galaxies (e.g. (6)), broad line radio galaxies (BLRG) and quasars have jets pointing close to the line of sight, while narrow line radio galaxies (NLRG) have jets closer to the plane of the sky. Cygnus A is a NLRG, and Pictor A is a BLRG, suggesting again that Pictor A is aligned closer to the line of sight.

2 Collective X-ray–detected hotspot properties; A Unified Picture

We examine here the properties of the X-ray detected hotspots in relation to the orientation of their jets relative to the line of sight. In table 1 we present the sources with X-ray hotspot detections, their emission line classification, core dominance R , their optical and X-ray hotspot properties, and the possibility of modeling their spectra with SSCE. An orientation sequence emerges from these observations: as the jet aligns closer to the line of sight, measured by an increase in R , the source changes from a NLRG to a BLRG/Quasar. Sources closer to the plane of the sky show X-ray hotspots in both lobes (except for the peculiar radio galaxy 3C 123, where only one hotspot is detected (12)), while more aligned sources show X-ray hotspots only on the side of the near jet, as identified through VLBI observations. While in NLRG, SSCE models are in agreement with the observed X-ray flux, in the more aligned BLRG

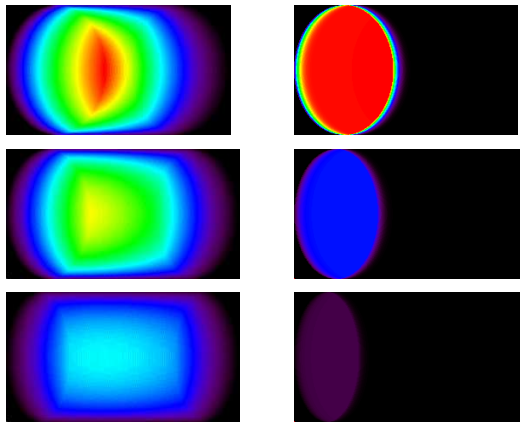


Fig. 1. Maps of radio (left) and optical (right) emission under observing angles of 40° (top), 50° (middle), and 60° (bottom) from a relativistic decelerating flow.

and quasars, the X-ray emission from the hotspot is brighter than the SSCE predicted flux, and one has to resort to magnetic fields well below equipartition (by a factor of $\sim 10 - 30$) to reproduce the observed X-ray flux (except for 3C 263, where reproducing the X-ray flux requires a magnetic field half of the equipartition value(8)). Synchrotron optical emission, weak or absent for the NLRG hotspots, appears at the jet side hotspot as the source aligns closer to the line of sight. Finally, radio emission is present in both hotspots, regardless of orientation, although the hotspot in the jet side of BLRGs and quasars is more powerful and has a flatter spectrum.

This orientation sequence suggests that the synchrotron emission be beamed, with the beaming increasing with frequency. The synchrotron optical emission is strongly beamed, and in the more aligned objects it is seen in the hotspot of the near jet. The radio emission is less beamed, as both radio hotspots are seen in all objects. Increase in alignment leads also to an increase in the hotspot X-ray-to-radio ratio, from the SSCE to larger values, indicating the presence of an additional component more sensitive to orientation effects than the IC component of SSCE. We suggest that this frequency dependent beaming results from a relativistic and decelerating flow at the hotspots. Such hotspot flow patterns with Lorentz factors up to $\Gamma \sim 3 - 4$ are routinely seen in relativistic hydrodynamic simulations (20; 21), and have been used (21) to explain the fact that, in the radio regime, the near hotspots are more powerful and have a flatter spectrum than the far ones.

We show in figure 1 the optical and radio maps of a kinematic one-dimensional model for the hotspot flow. Particle acceleration takes place at the shock front at the base of the flow. Electrons are advected downstream loosing energy due to radiative losses, while the bulk flow velocity decelerates to match the sub-relativistic advance speed (22) of the hotspots. The most energetic electrons are located closer to the fast base of the flow and their synchrotron emission

(mostly optical) is strongly beamed, seen preferentially in the near hotspot of the more aligned sources. The radio emission comes from the less energetic electrons, further downstream where the flow is slower, resulting in a wider beaming pattern, thus detected at a wider range of angles. The SSC emission responsible for the X-ray flux (not shown in figure 1; work in progress) does not follow the typical SSC/synchrotron beaming pattern. Because the fast electrons at the base of the flow see the radio emission of its slower, upstream sections as external radiation, the SSC beaming pattern is more focused than the synchrotron one and the radio-to-X-ray flux ratio increases as the source aligns to the line of sight, while it would remain constant within standard SSC process, in support of the slowing-down relativistic flow proposal.

References

- [1] Harris, D. E., Carilli, C. L. & Perley, R. A. *Nature* **367**, 713 (1994)
- [2] Wilson, A. S., Young, A. J. & Shopbell, P. L. *ApJ* **544**, L27 (2000)
- [3] Wilson, A. S., Young, A. J. & Shopbell, P. L. *ApJ* **547**, 740 (2001)
- [4] Tingay, S. J. et al. *AJ* **119** 1695 (2000)
- [5] Zirbel, E. L. & Baum, S. A. *ApJ* **448**, 521 (1995)
- [6] Urry, C. M. & Padovani, P. *PASP* **107**, 803 (1995)
- [7] Saikia D. J. & Kukarni V. K. *MNRAS* **270**, 897 (1994)
- [8] Hardcastle, M. J., et al. *ApJ* **581**, 948 (2002)
- [9] Harris, D. E., et al. *ApJ* **530**, L81 (2000)
- [10] Brunetti, G., Cappi, M., Setti, G., Feretti, L. & Harris, D. E. *A&A* **372**, 777 (2001)
- [11] Hardcastle, M. J., Alexander, P., Pooley, G. G. & Riley, J. M. *MNRAS* **296**, 445 (1998)
- [12] Hardcastle, M. J., Birkinshaw, M. & Worrall, D. M. *MNRAS* **323**, L17 (2001)
- [13] Hough, D. H., & Readhead, A. C. S. *AJ* **98**, 1208 (1989)
- [14] Wills, B. J. & Browne, I. W. A. *AJ* **302**, 56 (1986)
- [15] Brunetti, G. et al. *AJ* **561**, L157 (2001)
- [16] Lähteenmäki A. & Valtaoja, E. *AJ* **117**, 1168 (1999)
- [17] Kataoka, J., Edwards, P., Georganopoulos, M., Takahara, F. & Wagner, S. *A&A* (2003) (in the press); also as preprint astro-ph/0211514
- [18] Prieto, M. A. & Kotilainen, J. K. *ApJ* **491**, L77 (1997)
- [19] Prieto, M. A. *MNRAS* **284**, 627 (1997)
- [20] Aloy , M. A., Ibáñez , J. M., Martí, J. M., Gómez , J. L., & Müller, E. *ApJ* **523**, L125 (1999)
- [21] Komissarov, S. S., & Falle, S. A. E. G. In *ASP Conf. Ser. Vol. 100, Energy Transport in Radio Galaxies and Quasars*, (ed. P. E. Hardee, A. H. Bridle, & J. A. Zensus) 327 (ASP, San Francisco, 1996)
- [22] Arshakian, T. G. & Longair, M. S. *MNRAS* **311**, 846 (2000)